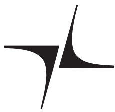

Special Feature: Power Semiconductor Devices

Research Report

Analysis of Dislocation Structure in Repeated *a*-face Grown Silicon Carbide Crystals

Itaru Gunjishima, Yasushi Urakami, Hiroyuki Kondo, Fusao Hirose, Ayumu Adachi, Shoichi Onda and Koichi Nishikawa

Report received on Aug. 6, 2015

ABSTRACT Morphologies of dislocations, such as orientation and linearity, in high quality SiC crystals, were analyzed by applying a two-dimensional fast Fourier transform (2D-FFT) to X-ray topographic images. The differences between an SiC crystal fabricated by a conventional repeated *a*-face (RAF) method and another fabricated by an improved RAF method with a lower dislocation density were investigated. The topographic images of basal plane dislocations (BPDs) obtained by $1\bar{1}00$ diffraction showed that the BPD density was much lower in the improved RAF crystal, and that the BPDs were highly oriented and linear, whereas BPDs in the conventional RAF crystals were complexly entangled. 2D-FFT images of the X-ray topographic images of the improved crystal showed bright lines toward the <$1\bar{1}00$>* directions that correspond to an orientation of the BPDs in the <$11\bar{2}0$> direction. This implies that the <$11\bar{2}0$> orientation is more stable for BPDs in SiC crystal, and the very low threading screw dislocation (TSD) density helped them to take that form. The degree of BPD orientation was quantified by deriving functions from the 2D-FFT images. The degree of orientation of the improved RAF crystal was 1.60, compared to 1.16 for the conventional RAF crystal. Therefore, the 2D-FFT process is a very effective method of analyzing and quantifying dislocation morphology in SiC crystals.

KEYWORDS Silicon Carbide, Single Crystal, Bulk Growth, Repeated *a*-face Method, RAF, Dislocation, X-ray Topography, Fourier Transformation

1. Introduction

Silicon carbide (SiC) is characterized, in comparison with Si, by a high thermal conductance, a wide band gap, and a high breakdown electric field strength. For that reason, SiC is a promising potential substitute for Si in next-generation power devices. However, SiC contains various types of dislocations that limit device performance. In particular, basal plane dislocations (BPDs) have recently become the next issue.

Many BPDs exist in the c-plane, and they generally have a complex morphology. Because they are complexly intertwined with threading screw dislocations (TSDs) in the <0001> direction, they can cause several problems. If the BPDs are curved in this way, and a substrate for device manufacturing is taken from a single crystal, a single BPD can be exposed at multiple sites on the surface of the substrate. As a result, the dislocation is succeeded from the plural sites when the epitaxial film is formed,(1) and the dislocation density in the epitaxial layer will increase relative to that of the substrate. Furthermore, BPDs oriented in a crystallographically unstable direction tend to decompose into stable partial dislocations,(2) which can degrade device performance. Needless to say, further reduction of BPDs is therefore important. Another approach to resolving those problems may be controlling the morphology of the BPDs. Linear and crystallographically stabilized BPDs are expected to minimize multiple TED generation and BPD decomposition.

It is possible to reduce the dislocation density in a crystal rapidly by using the repeated *a*-face (RAF) method in which *c*-face growth is performed after repeated *a*-face growth.(3) Furthermore, BPDs tend to be oriented by the RAF method.(4) However, the literature offers no obvious method of determining the orientation and linearity of BPDs in a crystal. Although an orientation tendency can be partially recognized in each dislocation, the linearity is not strong and many curved parts exist. In this study, we fabricated high quality SiC crystals using an improved RAF method (5) and performed two-dimensional fast Fourier transform (2D-FFT) analysis of X-ray topographic images

© Toyota Central R&D Labs., Inc. 2015

of BPDs to quantify the BPD morphology,[6] i.e., orientation and linearity.

2. Experimental

2. 1 Preparation

An SiC crystal was grown by the RAF method (see **Fig. 1**). First, a seed crystal with an *a*-face as the growth surface was cut from an SiC crystal with a high dislocation density. In this study, the first *a*-face seed had a $\{1\bar{1}00\}$ face as the growth surface, and the growth was conducted toward the $\langle 1\bar{1}00\rangle$ direction. Then, a $\{11\bar{2}0\}$ face seed was sliced from the $\{1\bar{1}00\}$ face grown crystal and second *a*-face growth was conducted in the $\langle 11\bar{2}0\rangle$ direction. After several repetitions of alternating *a*-face growth, a *c*-face seed crystal was cut out. Finally, *c*-face growth was conducted on the seed crystal. The *c*-face growth crystal was 1 inch in diameter. The number of *a*-face growth steps was increased, and the conditions for *a*-face and *c*-face growth were more optimal in the fabrication of the improved RAF crystal compared to the conventional RAF crystal.

2. 2 X-ray Topography and 2D-FFT Analysis of Topographic Images

After the *c*-face growth, a plate specimen was cut from the crystal almost parallel to the {0001} face to evaluate the crystal quality. The TSD density and BPD morphology were analyzed by reflection X-ray topography using $11\bar{2}8$ diffraction and transmission X-ray topography using $1\bar{1}00$ diffraction, respectively. A similar specimen from a previous study[4] was also measured. Then, the X-ray topographic images were analyzed using a 2D-FFT (see **Fig. 2**). For the $1\bar{1}00$ diffraction of the transmission X-ray topography, three crystallographically equivalent $1\bar{1}00$ diffractions, i.e., $\bar{1}010$, $1\bar{1}00$ and $01\bar{1}0$, were used to detect the BPDs. Two out of three BPDs could be imaged using $1\bar{1}00$ diffraction, because the dislocation contrast vanishes when the diffraction vector is perpendicular to the Burgers vector of the BPDs, as shown in **Fig. 3**. The three topographic images of the specimen were then digitized. The same square area was extracted from each image and analyzed using a 2D-FFT. The 2D-FFT resolves images into sine waves with certain frequencies and amplitudes (see Fig. 2). As shown in Figs. 2 and 3, if the lines in an image are highly oriented, the 2D-FFT image shows streaks perpendicular to the orientation direction of the lines.[7]

From the 2D-FFT images, functions expressing the degree of orientation were calculated (see Fig. 3).[7] The amplitude of the Fourier coefficient (A), which reflects the brightness of the 2D-FFT image, was averaged from the center of the image along radial directions (θ) from 0 to 180 degrees.[7] This process was carried out for each of the three 2D-FFT images, and the resulting $A_{ave}(\theta)$ values were summed to obtain $A'_{ave}(\theta)$, which reflects the actual BPD distribution. The degree of orientation, defined as the mean of the signal-to-noise ratio at peaks in $A'_{ave}(\theta)$, was then calculated.

3. Results and Discussion

3. 1 Observation of Dislocations by X-ray Topography

From the reflection X-ray topography using $11\bar{2}8$ diffraction, the TSD density of the improved RAF wafer in this study was determined to be 1.3/cm^2.

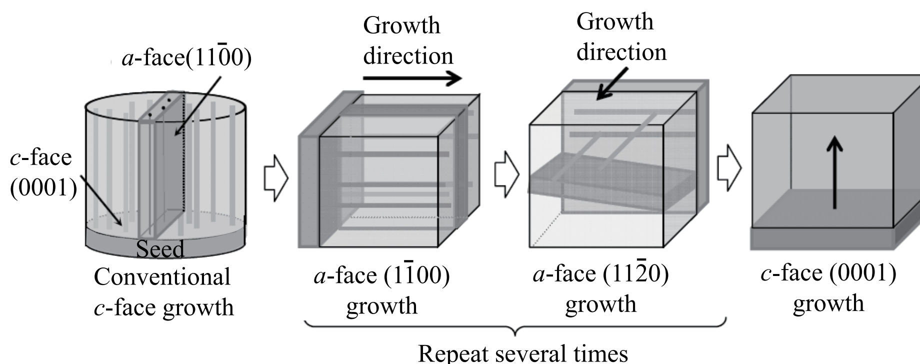

Fig. 1 Repeated *a*-face growth (RAF) method.

© Toyota Central R&D Labs., Inc. 2015

This value is more than one order of magnitude lower than that of the conventional RAF wafer. Owing to the increased number of *a*-face growth steps and the optimization of growth conditions, this low TSD density was achieved.

Figure 4 shows transmission X-ray topographic images of (a) $\bar{1}010$, (b) $1\bar{1}00$ and (c) $01\bar{1}0$ diffractions from identical areas of an improved RAF crystal and (d) $\bar{1}010$ diffraction from the conventional RAF crystal.(4) These 10 mm square images were extracted from the centers of the topographic images of the wafers. The three topographic images of the improved RAF wafer looked quite different, even though they were obtained from identical areas. As there are three different types of BPDs which are crystallographically equivalent but have Burgers vectors parallel to the $[1\bar{2}10]$, $[11\bar{2}0]$ or $[\bar{2}110]$ directions, a different third of the BPDs was undetected in each diffraction image.

The BPD density of the RAF crystal in this study was approximately one-fifth that of the conventionally grown RAF crystal. This low BPD density made the determination of the shapes and lengths of individual BPDs easier than for the conventional RAF crystal. In the images of the improved RAF wafer, there was almost no entanglement of the dislocations, and the BPDs were long and linear. This may have been due to the extremely low TSD density. BPDs and TSDs are almost perpendicular to each other in an SiC crystal. If BPDs migrate among the TSDs for some reason such as thermal stress caused by a change in the temperature

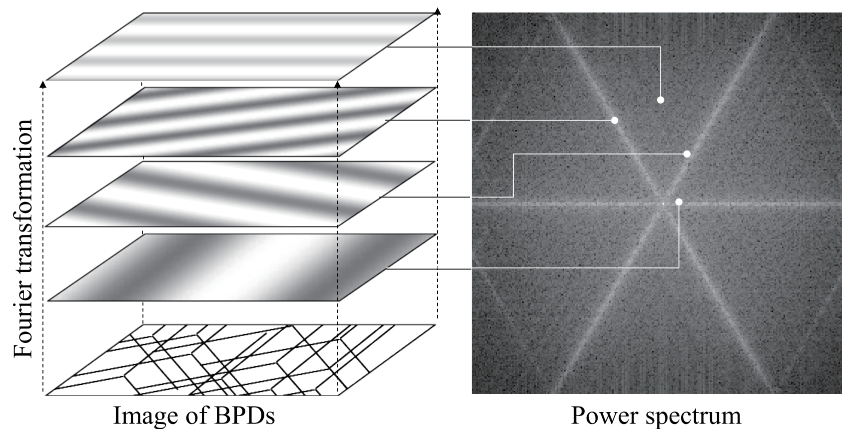

Fig. 2 Schematic illustration of 2D-FFT.

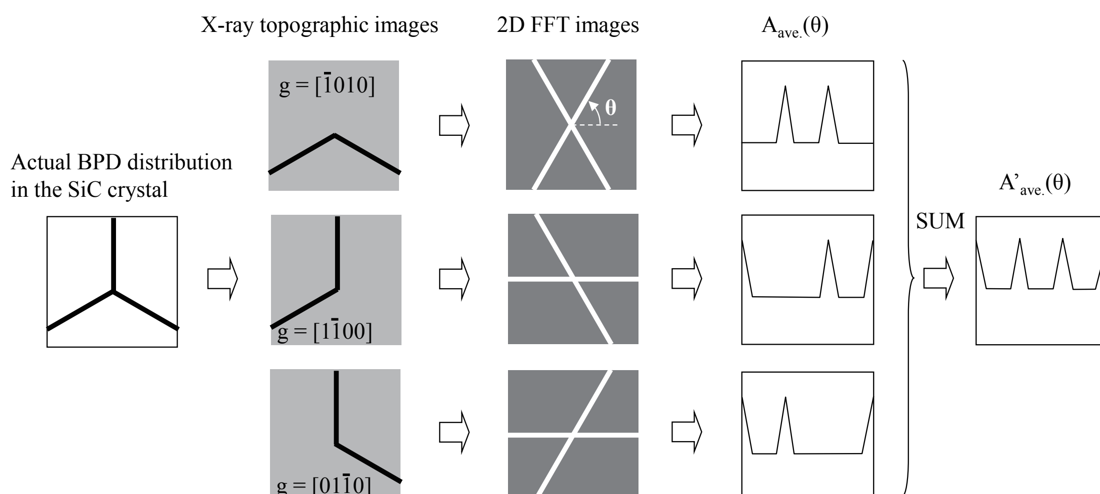

Fig. 3 Schematic illustration of the method used to obtain two-dimensional fast Fourier transform (2D-FFT) images of all BPDs. The center angle θ-dependence of the average amplitude of the Fourier coefficient (A) in the radial direction is shown.

© Toyota Central R&D Labs., Inc. 2015

distribution, pinning of BPDs by TSDs could occur, resulting in BPDs with a winding shape. Such pinning of BPDs by TSDs is extremely uncommon in the improved RAF crystal with an extremely low TSD density. The linear BPDs observed in this study can only intersect with a crystal surface at a single site. Therefore, multiple TED generation from multiple exposed sites of a single BPD on a substrate surface can be avoided when the epitaxial layer is formed.

3. 2 2D-FFT Analysis of the Dislocation Morphology

Figure 5 shows 2D-FFT images obtained from the X-ray topographic images in Fig. 4. The influence on the 2D-FFT images of changing the contrast of the topographic images or the size of the measurement region was also investigated. However, the 2D-FFT images were not influenced by contrast change of the X-ray topographic images, because the 2D-FFT process detects only the periodicity of the images. When the size of the measurement region was increased from 10 mm square to 20 mm square, the 2D-FFT images became unclear. This is because the BPD images became so fine in the topographic images that they were not detected in the 2D-FFT process at the selected resolution. Therefore, an appropriately sized measurement region or an appropriate resolution of 2D-FFT should be selected.

In Figs. 5(a), (b) and (c), clear lines can be recognized in the directions corresponding to the $\langle 1\bar{1}00\rangle^*$ direction, indicating strong $\langle 11\bar{2}0\rangle$ orientations for the BPDs. In contrast, as shown in Fig. 5(d), no clear line was recognized in the directions corresponding to the $\langle 1\bar{1}00\rangle^*$ direction in the 2D-FFT image obtained from the conventional RAF crystal, and only a weak variation in contrast with changing radial angle was observed. These results suggest that the $\langle 11\bar{2}0\rangle$ directions are more stable for BPDs in SiC crystals, and that the crystal produced in this study had a larger portion of such stabilized BPDs than the conventional RAF crystal. Since BPDs with Burgers vectors of a different two out of the three orientations were detected in each X-ray topographic image, different pairs of streaks oriented along the $\langle 1\bar{1}00\rangle^*$ directions appeared in each 2D-FFT image of the crystal produced in this study.

$A_{ave}(\theta)$ for each of the 2D-FFT images in Fig. 5 is

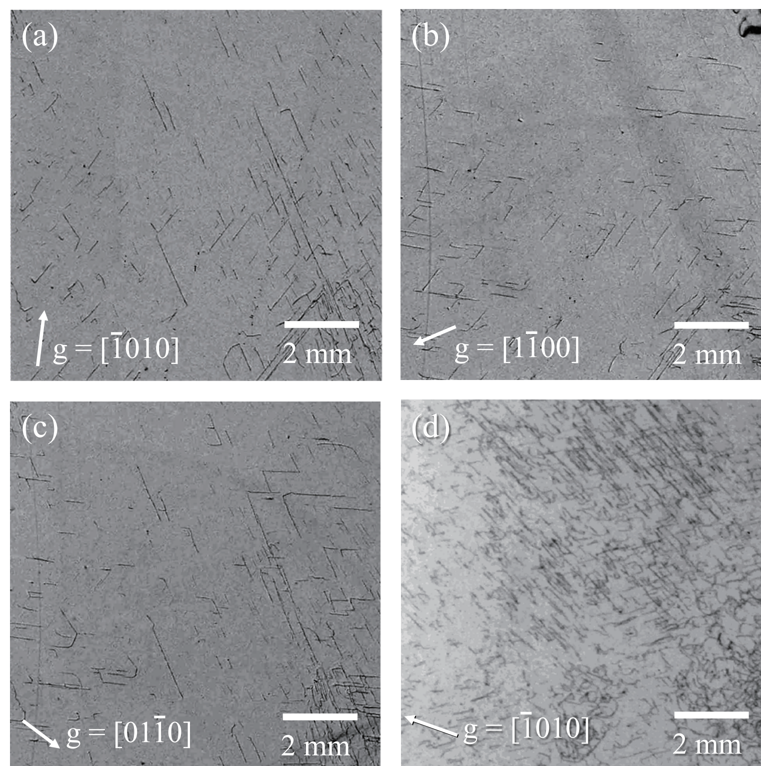

Fig. 4 X-ray topographic images of the RAF crystal grown in this study using (a) $\bar{1}010$, (b)$1\bar{1}00$ and (c) $01\bar{1}0$ diffractions, and that of conventional RAF crystal using $\bar{1}010$ diffraction.

© Toyota Central R&D Labs., Inc. 2015

shown in **Fig. 6**. For the RAF crystal produced in this study, two strong peaks were observed due to the streaks in the 2D-FFT images. The values of θ at these peaks correspond to the $\langle 1\bar{1}00\rangle^*$ directions. In contrast, $A_{ave}(\theta)$ for the previous RAF crystal exhibited no strong peaks, as shown in Fig. 6(d).

Figure 7 shows $A'_{ave}(\theta)$, which is the sum of the three $A_{ave}(\theta)$ curves from Figs. 6(a), (b) and (c). The signal-to-noise ratio at the peaks was 1.68 at $[\bar{1}100]^*$, 1.45 at $[\bar{1}010]^*$, and 1.56 at $[01\bar{1}0]^*$. The degree of orientation was high, with a value of 1.56. This indicates that the BPDs in the improved RAF crystal were highly oriented along three $\langle 11\bar{2}0\rangle$ directions. On the other hand, the degree of orientation calculated for the conventional RAF crystal was only 1.16. This indicates that the orientation of BPDs in the $\langle 11\bar{2}0\rangle$ direction was low.

Owing to the high linearity of the BPDs, the degree of orientation for the improved RAF crystal was larger than that for the conventional RAF crystal. This result demonstrates that the 2D-FFT process is a very effective method of analyzing and quantifying BPD morphology in SiC crystals.

4. Summary

In this study, we succeeded in fabricating SiC crystals with an extremely low TSD density of 1.3/cm^2 in a 1-inch region, and this low TSD density led to a characteristic BPD morphology. The orientation and linearity of BPDs in SiC crystals can be quantified using 2D-FFT analysis. The orientation of BPDs can be determined from the appearance and direction of lines in the 2D-FFT images of topographic BPD images. The linearity of the BPDs is reflected in the peak strength of $A_{ave}(\theta)$, which is the dependence of the amplitude of the Fourier coefficient on the crystallographic direction. The results of the 2D-FFT analysis indicated that improving the RAF method can result in BPDs that are more crystallographically stable and more linear. We showed a new approach to quantify dislocation morphology in SiC crystals by applying the 2D-FFT process to the evaluation of dislocations in crystals.

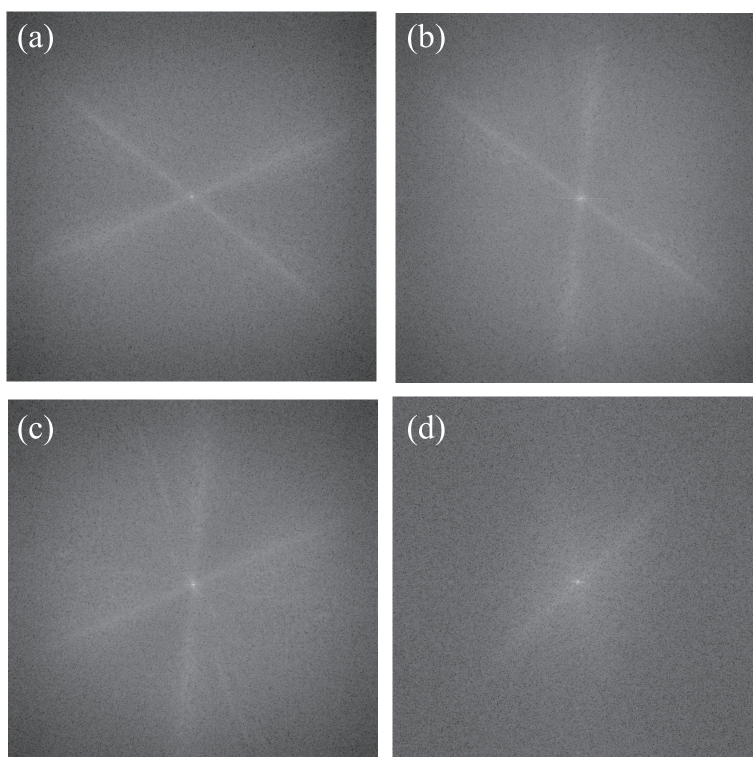

Fig. 5 2D-FFT images of X-ray topographic images of improved RAF crystal from this study using (a) $\bar{1}010$, (b)$1\bar{1}00$ and (c) $01\bar{1}0$ diffractions, and that of a conventional RAF crystal using $\bar{1}010$ diffraction.

© Toyota Central R&D Labs., Inc. 2015

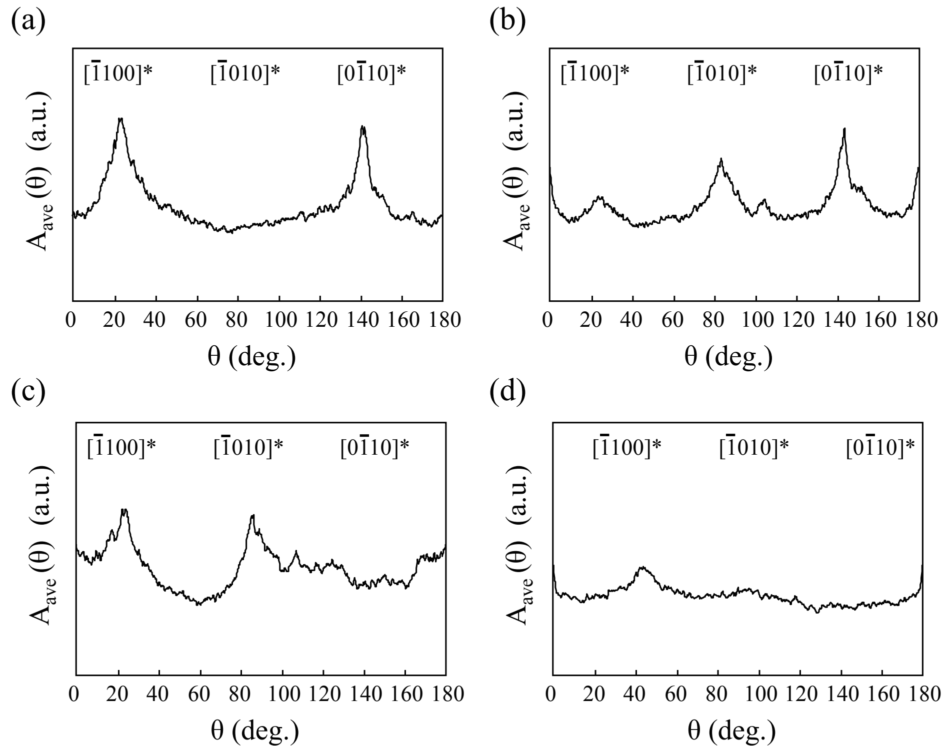

Fig. 6 $A_{ave}(\theta)$ of X-ray topographic images of the RAF crystal from this study using (a) $\bar{1}010$, (b) $1\bar{1}00$ and (c) $01\bar{1}0$ diffractions, and that of a conventional RAF crystal using $\bar{1}010$ diffraction.

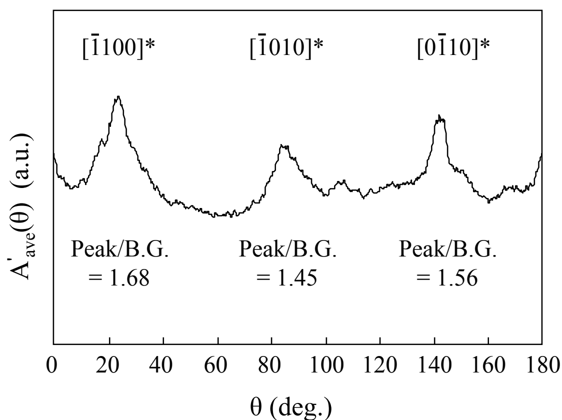

Fig. 7 Sum of $A_{ave}(\theta)$ from three X-ray topographic images (Figs. 5(a), (b) and (c)) of RAF crystal from this study.

Acknowledgements

This study was supported in part by Novel Semiconductor Power Electronics Project Realizing Low Carbon Emission Society of Japan Ministry of Economy, Trade and Industry (METI) and New Energy and Industrial Technology Development Organization (NEDO) through R&D Partnership for Future Power Electronics Technology (FUPET).

References

(1) Kamata, I., Nagano, M. and Tsuchida, H., "Characterization of Basal Plane Dislocations in 4H-SiC Substrates by Topography Analysis of Threading Edge Dislocations in Epilayers", *Mat. Sci. Forum*, Vol. 645-648 (2010), pp. 303-306.

(2) Stahlbush, R. E., Myers-Ward, R. L., VanMil, B. L., Gaskill, D. K. and Eddy, C. R., "A Pictorial Tracking of Basal Plane Dislocations in SiC Epitaxy", *Mat. Sci. Forum*, Vol. 645-648 (2010), pp. 271-276.

(3) Nakamura, D., Gunjishima, I., Yamaguchi, S., Ito, T., Okamoto, A., Kondo, H., Onda, S. and Takatori, K., "Ultrahigh-quality Silicon Carbide Single Crystals", *Nature*, Vol. 430 (2004), pp. 1009-1012.

(4) Nakamura, D., Yamaguchi, S., Gunjishima, I., Hirose, Y. and Kimoto, T., "Topographic Study of Dislocation Structure in Hexagonal SiC Single Crystals with Low Dislocation Density", *J. Crystal Growth*, Vol. 304 (2007), pp. 57-63.

(5) Urakami, Y., Gunjishima, I., Yamaguchi, S., Kondo, H., Hirose, F., Adachi, A. and Onda, S., "TSD Reduction by RAF (Repeated *a*-face) Growth Method", *Mat. Sci. Forum*, Vol. 717-720 (2012), pp. 9-12.

(6) Gunjishima, I., Urakami, Y., Hirose, F., Adachi, A., Onda, S. and Nishikawa, K., "Fourier Transform Analysis of Basal Plane Dislocation Structure in Repeated *a*-face Grown Crystals", *Mat. Sci. Forum*, Vol. 717-720 (2012), pp. 319-322.

© Toyota Central R&D Labs., Inc. 2015

(7) Enomae, T., Han, Y.-H. and Isogai, A., "Fiber Orientation Distribution of Paper Surface Calculated by Image Analysis", *Proc. Int. Papermaking and Environment Conf.* (*Tianjin, P. R. China*), Book2 (2004), pp. 355-368.

Fig. 1
Reprinted from Materials Science Forum, Vol. 717-720 (2012), pp. 9-12, Urakami, Y., Gunjishima, I., Yamaguchi, S., Kondo, H., Hirose, F., Adachi, A. and Onda, S., TSD Reduction by RAF (Repeated *a*-Face) Growth Method, © 2012 Trans Tech Publications Inc., with permission from Trans Tech Publications Inc.

Figs. 2, 3, 5-7
Reprinted from Materials Science Forum, Vol. 717-720 (2012), pp. 319-322, Gunjishima, I., Urakami, Y., Hirose, F., Adachi, A., Onda, S., Nishikawa, K., Fourier Transform Analysis of Basal Plane Dislocation Structure in Repeated *a*-face Grown Crystals, © 2012 Trans Tech Publications Inc., with permission from Trans Tech Publications Inc.

Text
Partially reprinted from Materials Science Forum, Vol. 717-720 (2012), pp. 319-322, Gunjishima, I., Urakami, Y., Hirose, F., Adachi, A., Onda, S., Nishikawa, K., Fourier Transform Analysis of Basal Plane Dislocation Structure in Repeated *a*-face Grown Crystals, © 2012 Trans Tech Publications Inc., with permission from Trans Tech Publications Inc.

Itaru Gunjishima
Research Fields:
- Inorganic Materials
- Crystal Growth
Academic Degree: Dr.Eng.
Academic Society:
- The Japan Society of Applied Physics

Yasushi Urakami*
Research Field:
- Research and Development of Power Devices of Silicon Carbide
Academic Society:
- The Japan Society of Applied Physics

Hiroyuki Kondo*
Research Field:
- Research and Development of Silicon Carbide Single Crystal Growth
Academic Society:
- The Japan Society of Applied Physics

Fusao Hirose*
Research Field:
- Research and Development of Next-generation Power Electronic Materials and Application
Academic Societies:
- The Japan Society of Applied Physics
- The Japan Institute of Metals and Materials

Ayumu Adachi**
Research Field:
- Management of Research and Development
Academic Society:
- Society of Automotive Engineers of Japan

Shoichi Onda*
Research Field:
- Research and Development of Silicon Carbide Semiconductor
Academic Degree: Dr.Eng.
Academic Society:
- The Japan Society of Applied Physics

Koichi Nishikawa
Research Field:
- Semiconductor Devices and Related Materials
Academic Degree: Dr.Eng.
Academic Societies:
- The Japan Society of Applied Physics
- The Japan Institute of Metals and Materials
- Society of Automotive Engineers of Japan

* DENSO CORPORATION
** Toyota Motor Corporation